Mine Closure 2022 - M Tibbett, AB Fourie & G Boggs (eds)

doi:10.36487/ACG_repo/2215_34

Advanced numerical modelling for closure work assistance

SH Lines *Red Earth Engineering, Australia*

M Llano-Serna *Red Earth Engineering, Australia*

Abstract

An internal bund was constructed for surface water management during the progressive closure of a tailings storage facility in northern Australia. Shortly after construction, and coinciding with the wet season's onset, significant longitudinal cracking was observed during routine visual inspections. Initial investigations involved more detailed visual inspections and satellite survey imagery to construct a timeline of events. Following this, three survey prisms were installed. Deformation modelling was complete to ascertain the extent of the cracking and settlement to establish potential ongoing and future consequences. The deformation modelling was conducted using Optum G2 with the modified cam-clay constitutive model being implemented based on the critical state concept. Model properties were derived from existing laboratory testing and field trials.

Preliminary modelling results were used to determine appropriate locations for the additional installation of six survey prisms at critical locations anticipated to experience significant movement. Furthermore, vertical settlement recorded via survey prisms was utilised for model calibration and identification of the leading deformation mechanisms. Following calibration, the model was used to predict future settlement and to model several water management scenarios, such as incorporating potential decant pond increases and varying pumping capacity limits. The numerical model was instrumental in informing a management strategy for the closure works.

The case study described herein shows how the use of numerical modelling as a tool was successfully employed to allow for more informed decision-making. This was accomplished by assessing the performance of geotechnical structures; in this case, the structure being an internal bund. Confidence in the numerical model was gained by calibrating results early during the deformation process and later using partial results for forward predictions.

Keywords: *numerical analysis, modified cam-clay, deformation modelling*

1 Introduction

Modern mining practices produce vast amounts of tailings (waste byproducts) that can leave devastating environmental, social and economic legacies (Espinoza & Morris 2017), with a closure having the potential to require perpetual management. These tailings must be responsibly managed to minimise the legacy impacts inherited by future generations. This is becoming an ever-increasing concern for the industry as the volume of tailings being produced continues to increase over time (Bowker & Chambers 2015). Tailings are generally made up of clays and silts, often with very high moisture content due to the pumping requirements and favourable economics of pumping compared to alternative deposition methods (Williams 2021). Tailings are stored in engineered facilities that are planned, designed, constructed, operated, closed and maintained in the long-term post-closure period (Mining Association of Canada 2017). One important aspect to note is due to the fine particle size of the material stored, tailings storage facilities (TSFs) often continue to consolidate years to decades beyond cessation of deposition.

Furthermore, changing conditions beyond closure mean potential failure modes must be anticipated, with the behaviour of the TSFs based on these potential failure modes. Numerous post-closure failures have occurred due to events such as earthquakes or heavy rainfall. Heavy rainfall, a particular concern across northern Australia, has been identified as the trigger in 25% of global and 35% of European TSF failures (Hu et al. 2021; Rico et al. 2008).

Deformation modelling used as a means of predicting or confirming the potential behaviour of TSFs is an increasingly common method (Mánica et al. 2022) and is recommended in some instances according to international guidelines and standards such as the Australian National Committee on Large Dams (2019). These analyses should be based on constitutive models that incorporate the fundamental mechanics capable of simulating the problems being addressed. For this study, the modified cam-clay (MCC) method was used. The MCC method is based on the critical state concept and is one of the most widely used methods and reliable constitutive models in use throughout the industry (Utomo et al. 2009). However, a drawback to be noted is that the MCC method does produce conservative results when modelling overconsolidated clays (Bruschi et al. 2021).

For this case study, a TSF in northern Australia undergoing progressive closure had a temporary internal bund constructed for surface water management during closure earthworks activities. The TSF is approximately 24 m in height with a storage capacity of 23 million cubic metres. The internal bund (Figure 1) was constructed approximately 100 m upstream from the western embankment. Construction material was sourced from the adjacent beach, with additional hauled in from nearby construction activities. The material was track rolled in without additional compaction. A drain was excavated downstream of the internal bund, and the decant pond was located upstream. The purpose of the internal bund was to serve as a barrier to avoid potential pond overflows reaching the finished drain ahead of surface treatment.

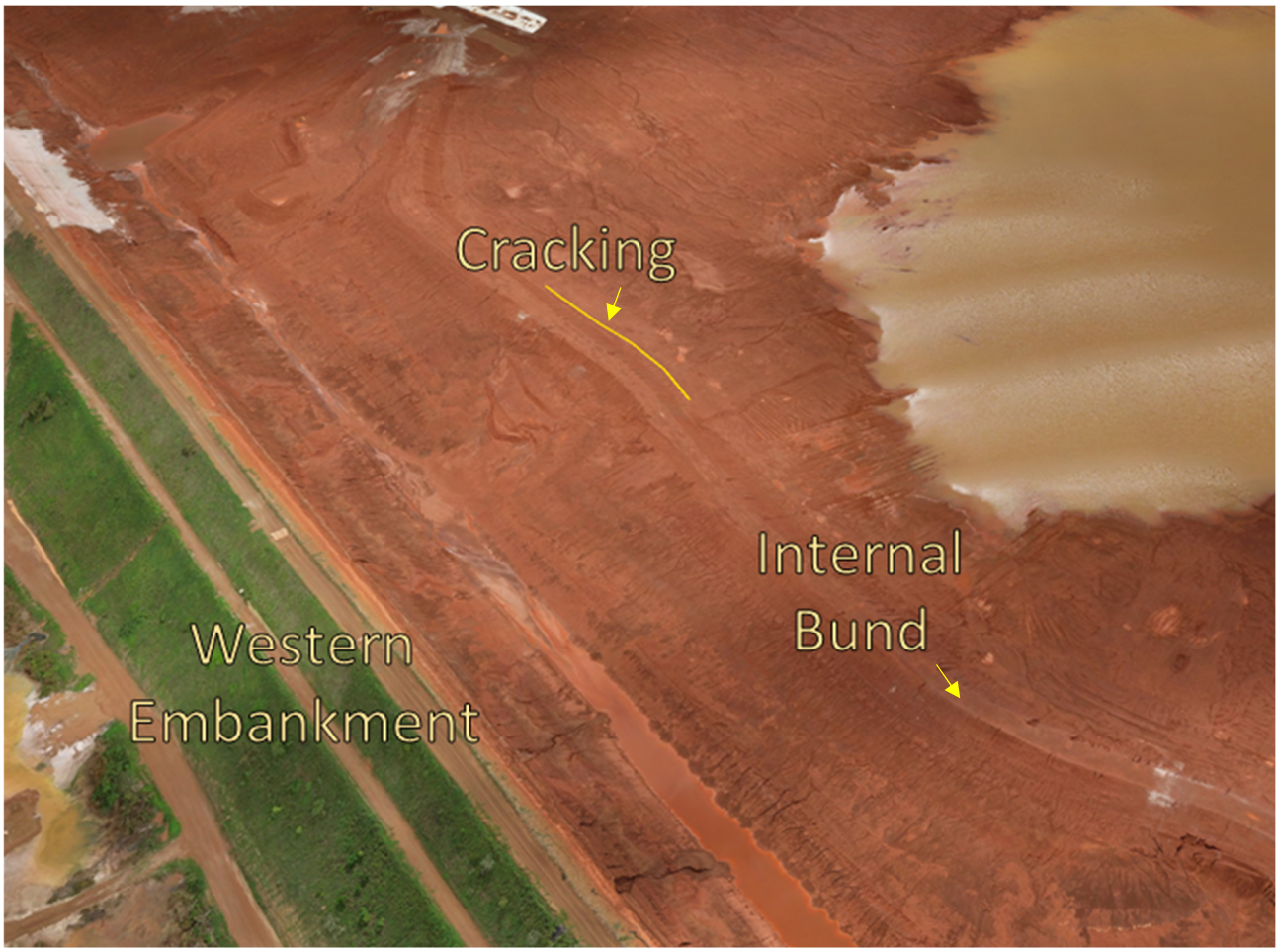

Figure 1 Snapshot of the TSF, including the closest embankment, internal bund and cracking location

The location of the TSF experiences a monsoonal climate, influenced by coastal factors, with hot, wet and humid summers and mild, dry winters. There is a distinct wet season from December to April whereby a vast majority of rainfall occurs, with the potential for tropical cyclones to form. The mean annual precipitation is approximately 1,500 mm. During a routine inspection on the 27th January 2022, cracking was noticed along the internal bund. The cracking was approximately 80 m in length and appeared upstream of the toe of the internal bund. Transversal cracking of approximately 6 m in length occurred south of the critical cross-section. This cracking led to the subsequent investigation, which included seepage and deformation modelling to assess the potential risks and consequences.

An aerial image of the internal bund on the 31st December 2021 is shown in Figure 2, with the cracking locations highlighted. Following the discovery of the cracking, a timeline was constructed using previous survey data to examine the settlement and construction in that location over time. Data were available as far back as 2018; however, it was not until mid to late 2021 that construction started to occur.

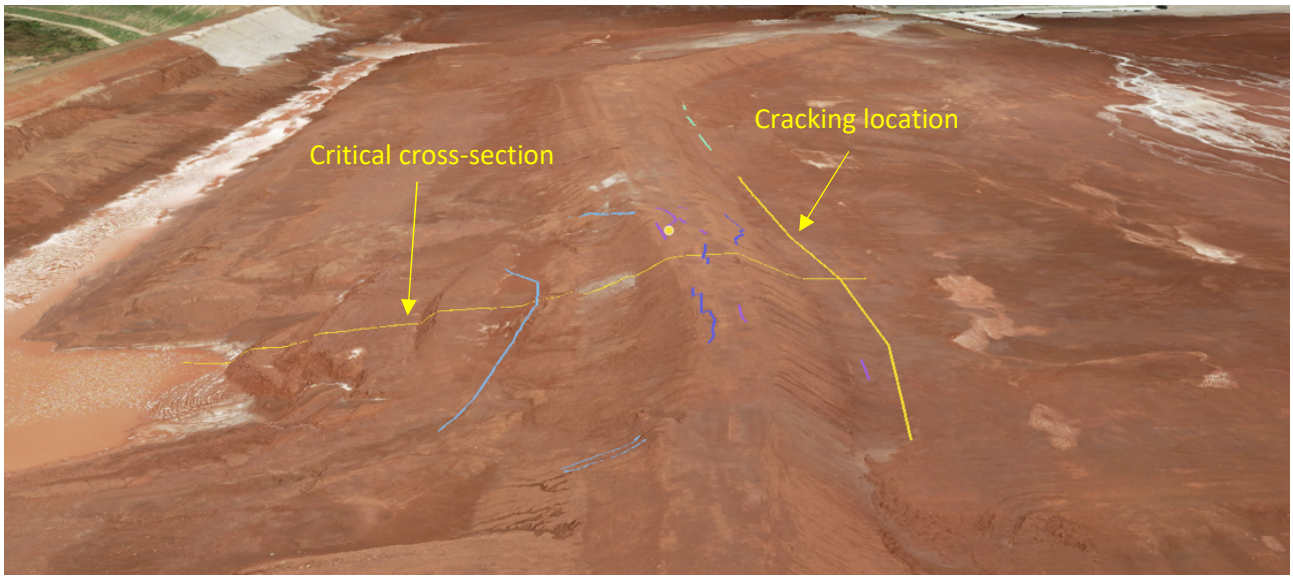

Figure 2 Internal bund after movement (31st December 2021) with cracking locations shown

Three key dates are shown in Figure 3; starting from the 29th September 2021, it can be seen there is a mound of loosely placed material approximately 2 m in height at Chainage 0–12 m. By 6th October 2021, this mound is removed, and the tailings are relatively flat. The survey on the 27th October 2021 reveals an excavation at a depth of approximately 2 m with a safety bund at approximately Chainage 0–15 m.

Figure 4 displays further development of the cross-section from the 27th October 2021 to the 3rd November 2021, including various points of interest and pertinent information regarding the tailings material. By this stage, further excavations (highlighted red) have taken place, and the internal bund has been built directly above the excavations. The previously mud-farmed tailings material (highlighted green) is located beneath the internal bund and has formed as a crust with increased strength related to the mud farming and desiccation. The cross-section was built using drone imagery, which is captured regularly onsite.

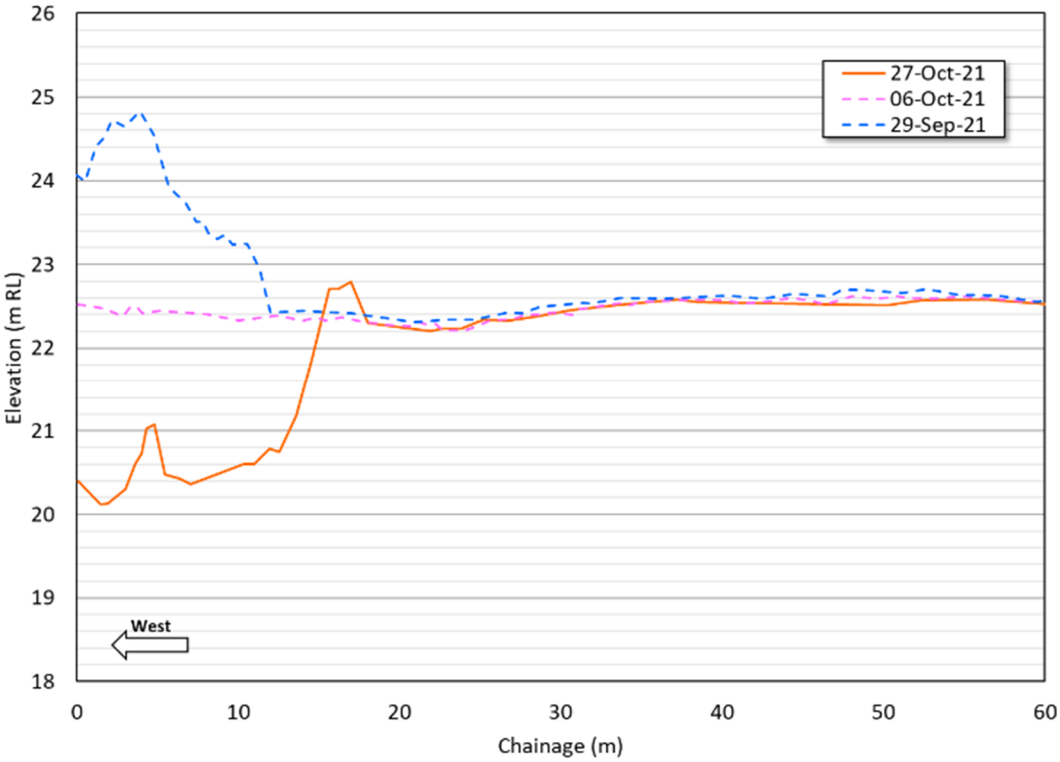

Figure 3 Cross-section view of the critical cross-section at various times throughout 2021

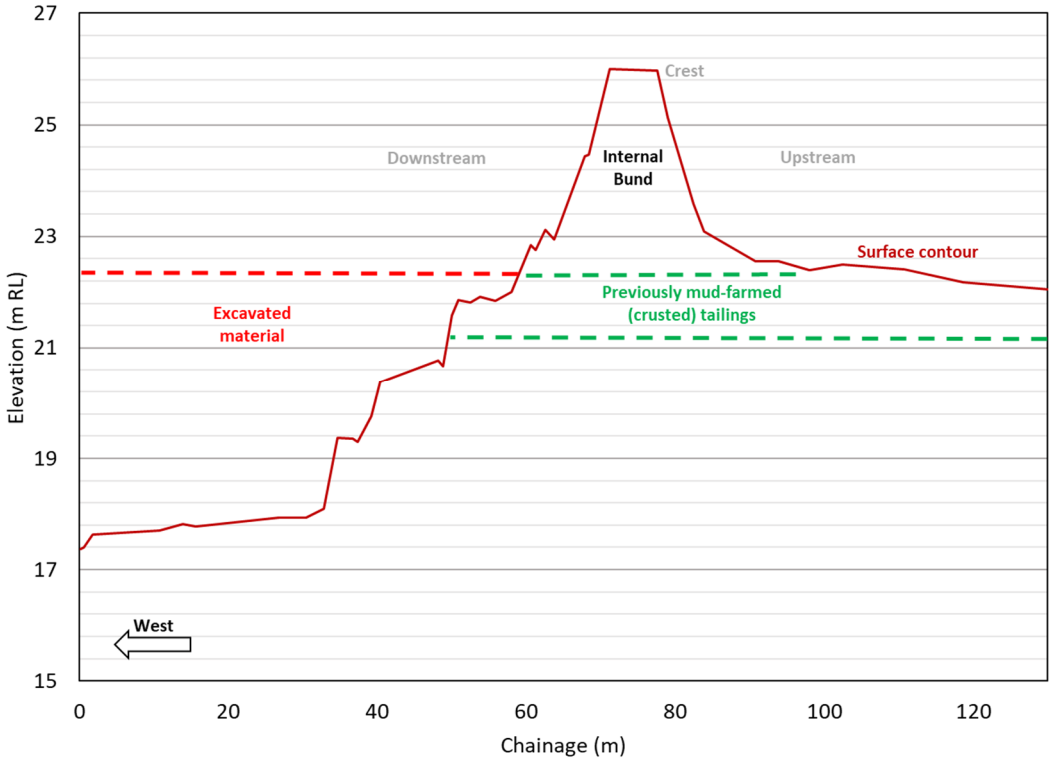

Figure 4 Cross-section of the internal bund, including points of interest

Upon discovery of the cracking, three survey prisms were installed along the bund crest to assess settlement over time. Readings were subsequently taken daily. The drone and prism results are shown in Figure 5. Monitoring data revealed primary consolidation took place before approximately 31st December 2021 and resulted in a vertical settlement of around 270 mm.

Subsequent creep consolidation took place and resulted in a further 240 mm settlement. Horizontal movements (not shown) indicated crest movement of approximately 13 mm, which was from a reduced period; however, it is noted that it is approximately 2.5% of the magnitude of the vertical displacement. Therefore, it is inferred that the governing movement mechanism is vertical displacement.

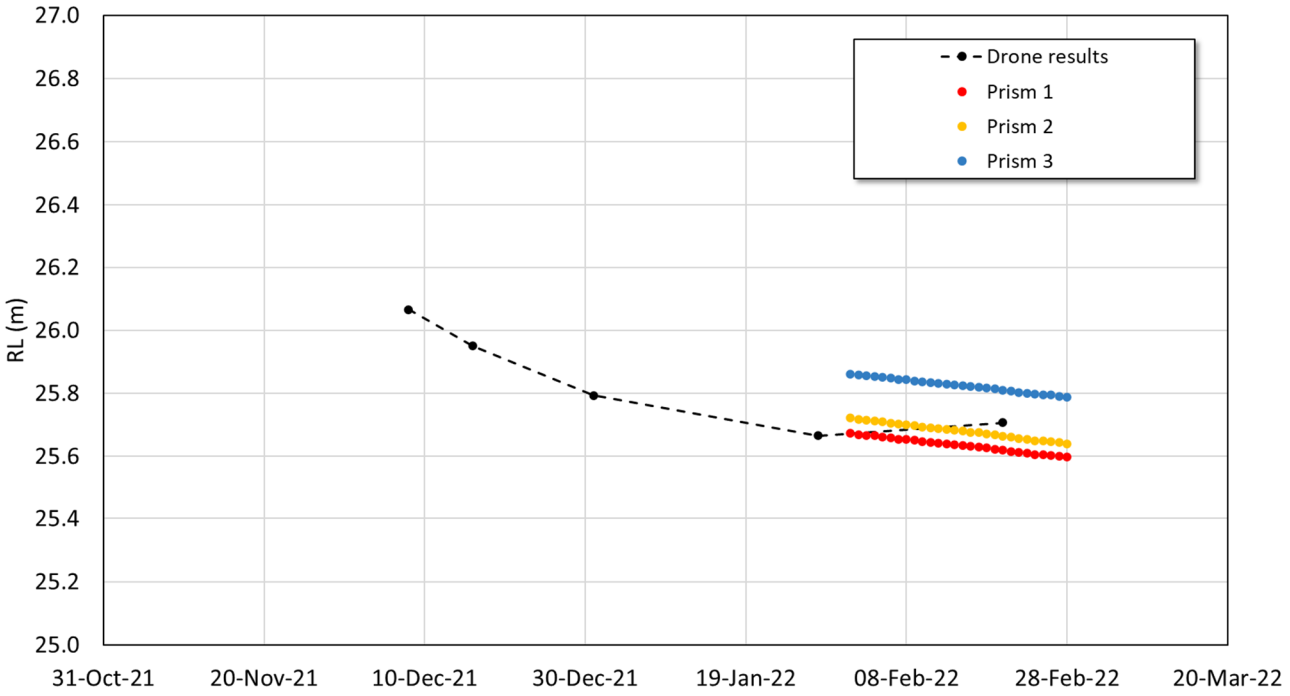

Figure 5 Survey prism settlement results compared to drone results

2 Methodology

2.1 Site characterisation

The characterisation was based on data from previous site investigations. The aim was to gather geotechnical, environmental and agronomy information and data in sufficient detail to support the proposed closure. The use of this data enabled a more informed model to be developed for forward-planning purposes. The tailings test results are shown in the subsequent section.

Figures 6 to 9 display the relevant soil parameters compared with the International Commission on Large Dams (2017) tailings classification criteria (CT: coarse tailings, HRT: hard-rock tailings, ART: altered rock tailings, FT: fine tailings, and UFT: ultrafine tailings). Most of the material can be classed as CT (from a grain-size perspective) of a medium plasticity clay with high plasticity silts (usually typical of finer tailings). The hydraulic conductivity was estimated indirectly from the oedometer tests and displays characteristics of a coarser material ranging from 1×10^{-9} m/s to 1×10^{-7} m/s. The oedometer results were used to develop the required parameters for the implementation of a MCC constitutive model.

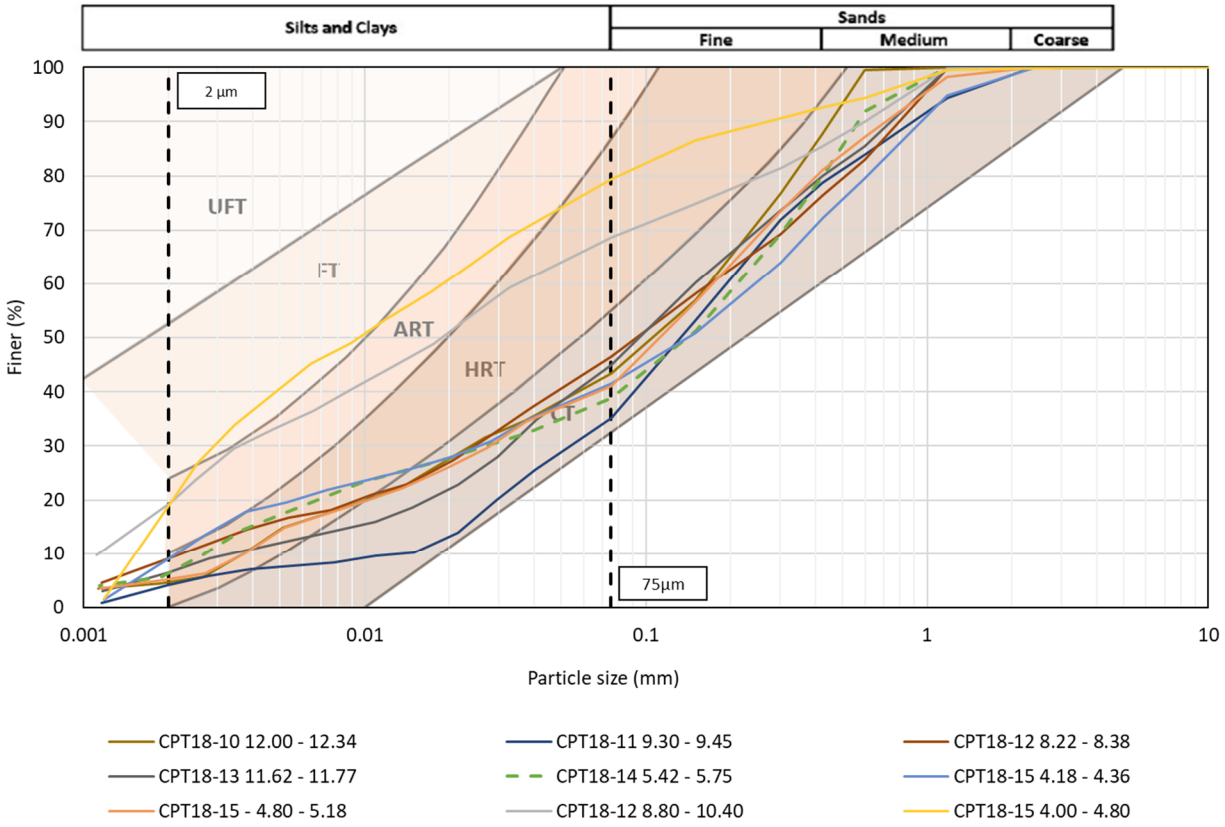

Figure 6 Particle size distribution results based on previous CPT investigation, overlaid tailings categories

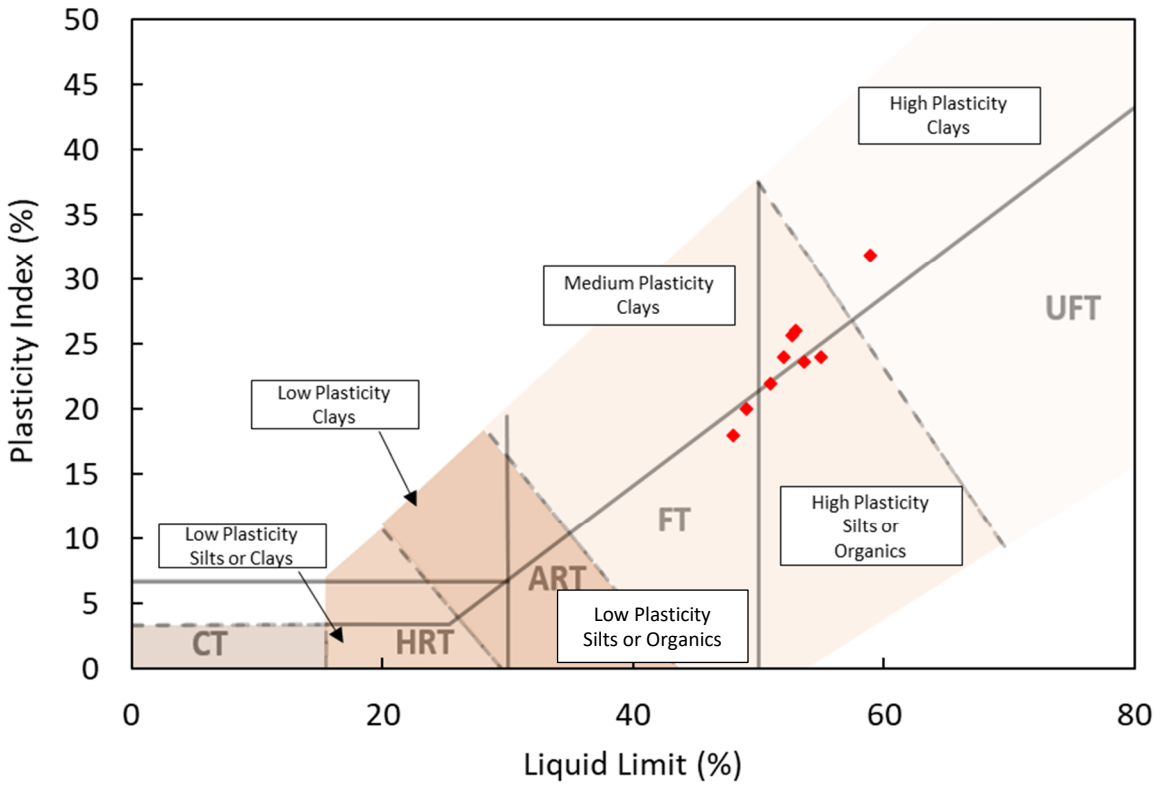

Figure 7 Atterberg limit results based on previous CPT investigation, overlaid tailings categories

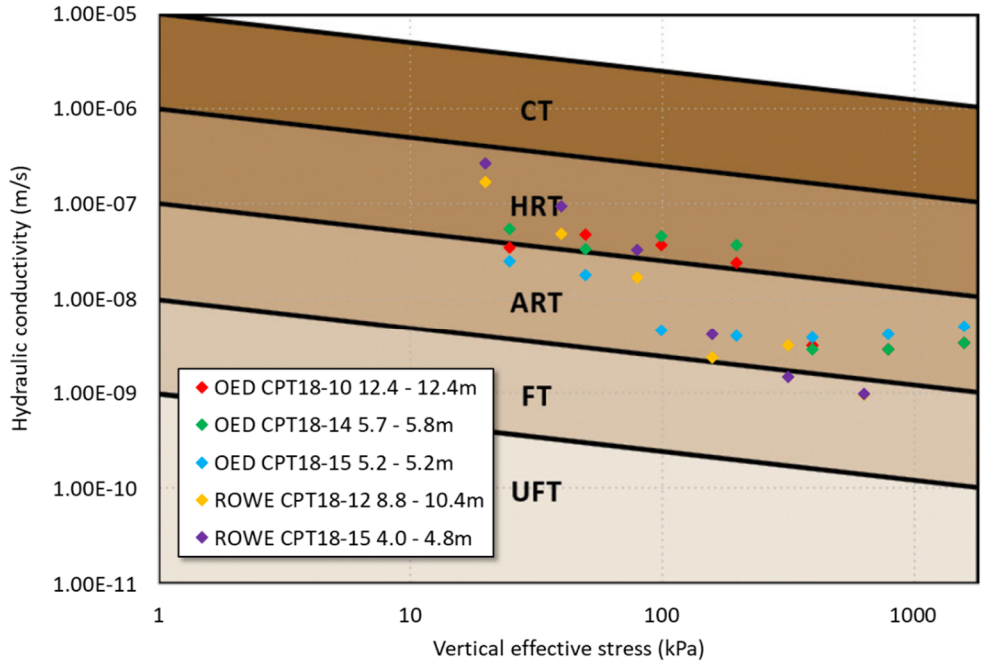

Figure 8 Hydraulic conductivity estimates based on oedometer test results, overlaid tailings categories

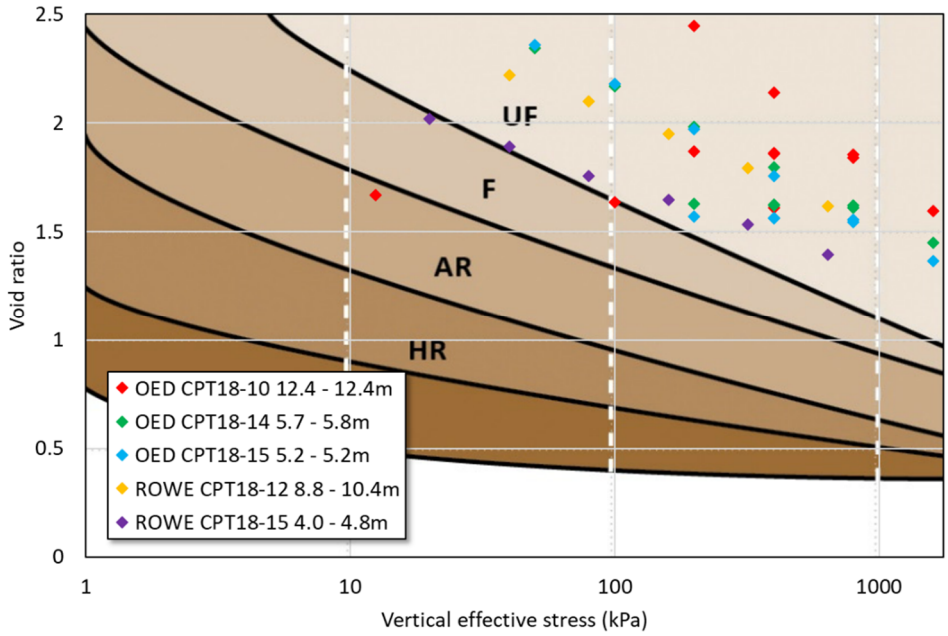

Figure 9 Oedometer test results (void ratio versus vertical effective stress), overlaid tailings categories

2.2 Parameter development

The tailings were split into four broad categories for modelling purposes:

- Tailings – the bulk of the material deposited over the life of the TSF.
- Tailings crust – formed since cessation of deposition, a thin layer across the TSF.
- Recently placed tailings – tailings relocated from the western section of the TSF and used to construct the internal bund.
- Remoulded tailings – tailings that have been loosely placed to fill on the downstream side of the internal bund.

2.2.1 Mohr–Coulomb

For tailings crust, recently placed tailings, and the remoulded tailings, the constitutive model Mohr–Coulomb (MC) was selected. The MC model is an elastic-perfect plastic model and widely used across the industry. It simulates a region of stress that can be reached elastically, whereby recovery of deformation is possible. However, further deformation beyond this point becomes irrecoverable.

2.2.2 Modified cam-clay

Settlement of the bulk of the tailings was modelled using the non-linear MCC constitutive model (Roscoe & Burland 1968). The MCC is an elasto-plastic model based on the critical state concept used to represent materials when the influence of volume change on bulk property and resistance to shear needs to be taken into consideration; an example would be soft and compressible clays. MCC can be described with four main parameters:

1. λ – Slope of the isotropic normal compression line (NCL) – see Figure 10 – developed based on oedometer tests conducted during previous site investigations.
2. κ – Slope of the recompression line (RL) – see Figure 10 – developed based on oedometer tests conducted during previous site investigations.
3. M – Slope of the critical state line in (p' – q) – estimates were based on site investigation CPT correlations (friction angles).
4. ν – Poisson's ratio – based on site experience with similar tailings.

In addition to the key parameters, creep (μ/λ) was also introduced due to the knowledge of ongoing creep being present. Initially, creep was estimated based on material properties using Mesri & Castro (1987); however, this estimate was further refined upon acquisition of the survey prism data. Tables 1 and 2 display the properties derived from laboratory testing based on the material categories.

Table 1 Mohr–Coulomb material properties

Material	Young's modulus E (MPa)	Poisson's ratio ν	Cohesion (kPa)	Friction angle (°)
Tailings – recently placed	15	0.25	2	32
Tailings – crust	25	0.25	25	2
Tailings – remoulded	35	0.25	5	32

Table 2 Modified cam-clay material properties

Material	Slope NCL κ	Slope RL λ	Poisson's ratio ν	Creep μ/λ	Cohesion (kPa)	Friction angle (°)
Tailings	0.016	0.413	0.35	5E-03	0	30

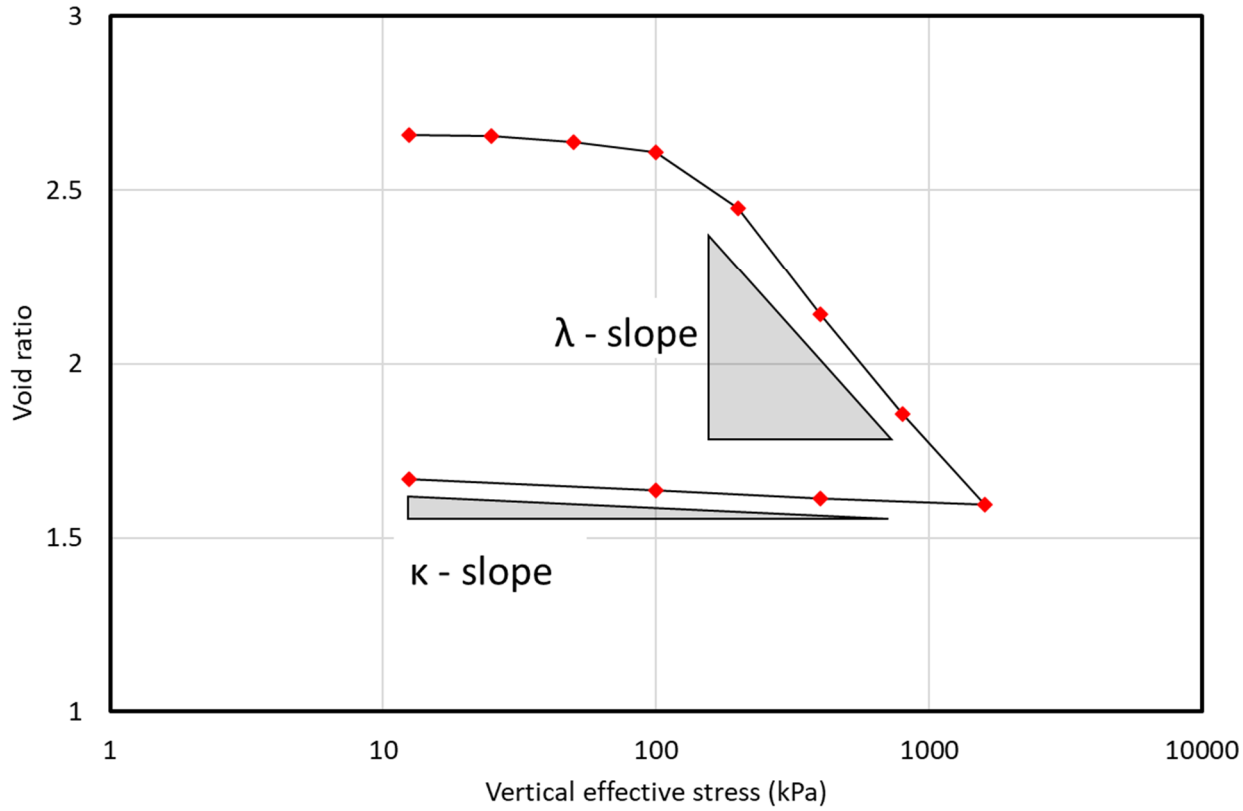

Figure 10 Oedometer results for OED CPT18-10 12.4–12.4 m displaying the source of kappa and lambda

2.3 Stage construction modelling

For both the seepage and the deformation analyses, construction was staged according to the history of the structure. Seepage modelling enabled more precise results of the porewater pressure build-up within the tailings, which resulted from the ongoing civil works (excavations, stockpile relocations and construction of the bund). The advantage of incorporating the construction sequence for deformation modelling was enabling a more accurate model regarding the stress history of the tailings material and the impact of loading and unloading over time.

2.4 Boundary conditions

2.4.1 Seepage analysis

There were two stages of model development. The initial stage was conducted using GeoStudio 2021.4 version 11.3.0, specifically the Seep/W module. Seep/W is a finite element package for the purposes of modelling groundwater flow in porous media, both saturated and unsaturated.

Seep/W was utilised with the available atmospheric data (obtained from both SILO and the onsite weather station) to compute the porewater pressures throughout the development of the internal bund, inclusive of the anticipated changes based on the wet season across 2021/2022. To complete this modelling, a steady-state analysis using a constant head boundary condition was set up, leading to a transient analysis with the land–climate interaction boundary condition being applied along the surface (Figure 11). Embankment faces were modelled as free surfaces to allow for potential seepage, and the saturated/unsaturated hydraulic material model was utilised with a Ky'/Kx' ratio of 0.67. The material was modelled as unsaturated/saturated and assigned parameters (such as hydraulic conductivity) based on the laboratory results outlined in Section 2.1. Mesh size was set to 0.5 m, with a total of 6,581 nodes and 6,384 elements used. The objective of this model was to understand the role of rainfall in the bund settling behaviour.

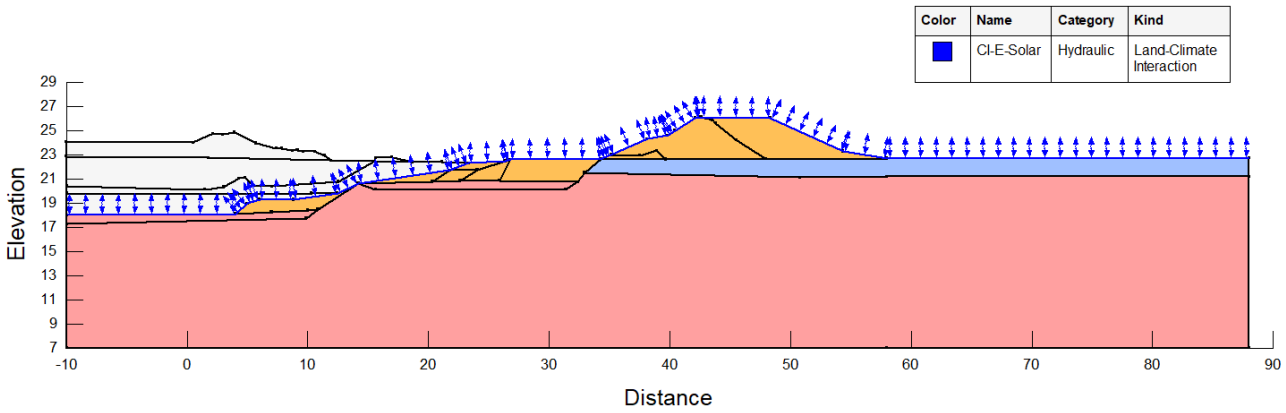

Figure 11 Cross-section of the TSF and internal bund with the land–climate interaction applied

2.4.2 Deformation

The software used for completing the consolidation assessment of the tailings was Optum G2 2021 version 2.1.6, a 2D finite element analysis (FEA) commercially available package capable of modelling compressibility problems with high efficiency. FEA allows discretisation of the area of investigation into a finite number of elements to create a mesh (Optum utilises triangular meshing). Each mesh element has a specific number of gauss points that are then used to compute stress and strain. Cross-sections of the internal bund were developed through the use of the regular surveys conducted by the site team.

The seepage results described in Section 2.4.1 were used as initial porewater pressures for model set-up. A linear elastic deformation relationship was adopted for all material types in the model, and a fixed boundary condition was assumed at the bottom of the model and far-field east and west. The model was extended and designed to ensure minimal influence of the boundary conditions on the internal bund (Figure 12). Mesh adaptivity was used with a total of 1,610 elements in the final model; convergence tolerance was set to 0.01 degrees. The objective of modelling was to determine the rate of settlement and projected settlement over time of the internal bund.

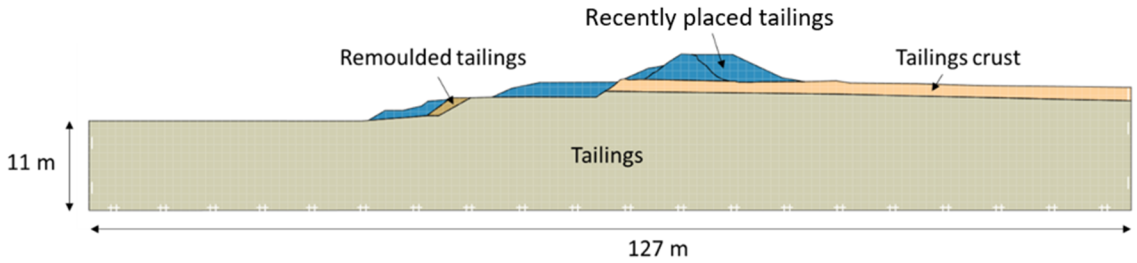

Figure 12 Cross-section of the internal bund on 28th February 2022

2.5 Predictive modelling

Four scenarios were developed and modelled in GoldSim to determine the decant pond elevation anticipated to develop throughout the wet season and leading into the 2022 dry season. Upon further review, this was refined down to two scenarios (Scenario 3 and 4), which were then investigated. Scenario 3 is presented within this report as it represents the most conservative.

List of scenarios:

1. Scenario 1 – Decant pond with two pumps, each running at 1,000 m^3/h.
2. Scenario 2 – Decant pond with two pumps, each running at 180 m^3/h.
3. Scenario 3 – Decant pond with one pump running at 180 m^3/h.
4. Scenario 4 – Decant pond with one pump running at 1,000 m^3/h.

The results are presented in Table 3, with the peak results for each scenario in **bold** and underlined text.

Table 3 Decant water level (m RL), monthly maximum, based on differing pumping capacities

	Scenario 1	Scenario 2	Scenario 3	Scenario 4
January	22.4	23.3	23.9	22.4
February	22.1	23.2	24.0	22.2
March	**22.3**	23.3	24.8	**22.5**
April	**22.3**	**23.5**	**25.1**	**22.5**
May	22.0	23.4	24.9	22.2
June	21.6	22.4	24.4	21.6
July	21.6	21.6	23.9	21.6
August	21.5	21.5	23.4	21.5
September	21.5	21.5	22.8	21.4
October	21.5	21.6	22.2	21.5
November	21.7	22.1	22.1	21.8
December	22.2	23.0	23.3	22.4

3 Results

The initial phreatic surface was estimated based on survey data over time, which was then used to set up a steady-state analysis. Following this, a subsequent transient analysis was set up using hydraulic conductivity values determined from laboratory testing (Table 4).

Table 4 Vertical hydraulic conductivity (m/s) to depth values adopted for modelling

Depth (m)	Hydraulic conductivity (m/s)
0–4	6.9E-08
4–6	3.5E-08
6–7	2.3E-08
7–16	1.2E-08
16+	5.8E-09

Figure 13 displays the porewater pressure within the tailings and internal bund on the 31st December 2021. This was following heavy rainfall over the Christmas period of approximately 350 mm over a four-day period. It can be seen that a drier initial crust formed at the surface of the tailings, with slight porewater pressure built up immediately below the areas of construction. The seepage analysis concluded that the effects of rainfall influenced the top 0.5 m of the tailings exposed to atmospheric conditions (displayed in the blown-up section of Figure 13). Furthermore, the model showed that for the period modelled between 8th December 2021 and 27th January 2022, the rainfall had a negligible influence on the position of the watertable. The model did not include water accumulation – that is, ponding upstream of the bund; the approach was considered adequate, as the decant pond was approximately 70 m away from the bund.

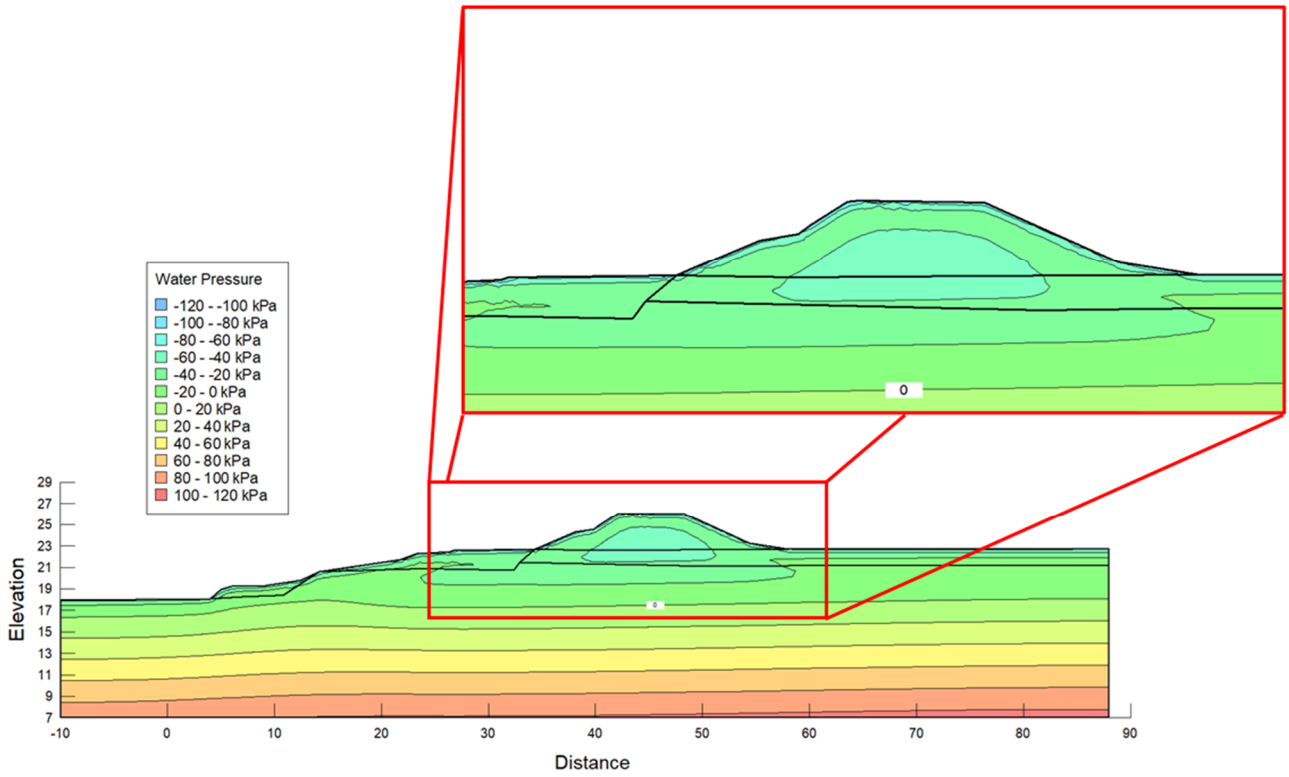

Figure 13 Porewater pressure results on the 31st December 2021

3.1 Deformation analysis results

Numerical modelling was completed both with and without creep. The results were compared to those observed from the survey prisms onsite to confirm the presence of creep. Calibration was undertaken using the slope of the survey prism results (a constant value based on creep), and it was determined that approximately 0.5 % creep exists. Mesri & Castro (1987) have reported that, for the majority of inorganic soft clays, the expected creep is approximately 4% (± 1%); the model presented herein indicates low creep magnitudes that are less than the rounding error reported in their paper. The Optum model was then extended, incorporating the maximum predicted decant pond elevation on the upstream side of the bund, using the levels determined through GoldSim modelling (refer to Section 2.5).

The deformation modelling results investigated the settlement of the internal bund within the western embankment. The main objective was to determine the trend, rate of settlement and anticipated total settlement. Figure 14 displays the anticipated saturation of the cross-section based on Scenario 3. It is noted that the saturation level is influenced by the water level of the decant pond, in addition to the material's hydraulic conductivity (both vertical and horizontal). The saturation modelling results indicate that the model overpredicts the phreatic elevation by around 1.0 m. Vibrating wire piezometers confirmed the modelling assumption installed around 150 m southwest of the critical cross-section compared well to a location of seepage recently observed further south along the bund.

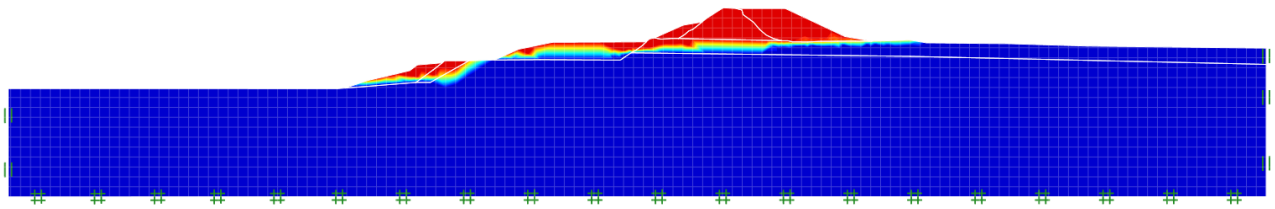

Figure 14 Saturation results of the internal bund; blue saturated and red unsaturated

Figure 15 shows the total displacement (mm) results for the internal bund from the 3rd November 2021 until the 30th March 2022. The internal bund itself displays the most significant total displacement at approximately 0.55 m at the ground surface (since construction). An increase in displacement radiates outwards from the internal bund towards the downstream portion of the cross-section.

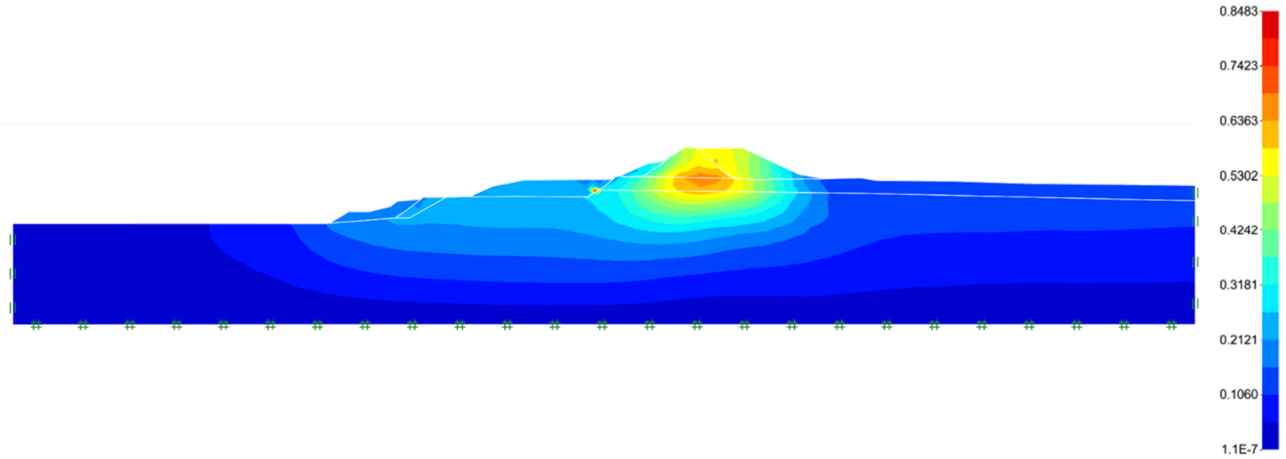

Figure 15 Colormap showing total displacement predictions (m) calculated with Optum for the internal bund until 30th March 2022

Figure 16 displays the results and shows a comparison between modelled vertical displacements at the crest of the bund, measured vertical displacements by prisms installed at the bund crest (averaged between the three crest prisms), and the predicted maximum pond level for Scenario 3 (worst-case scenario). Note that at the maximum decant water level (early April), the modelling shows there is approximately 500 mm freeboard for the internal bund. Thereafter, the water level drops significantly faster than the settlement, with the conclusion that freeboard will continue to increase throughout the year.

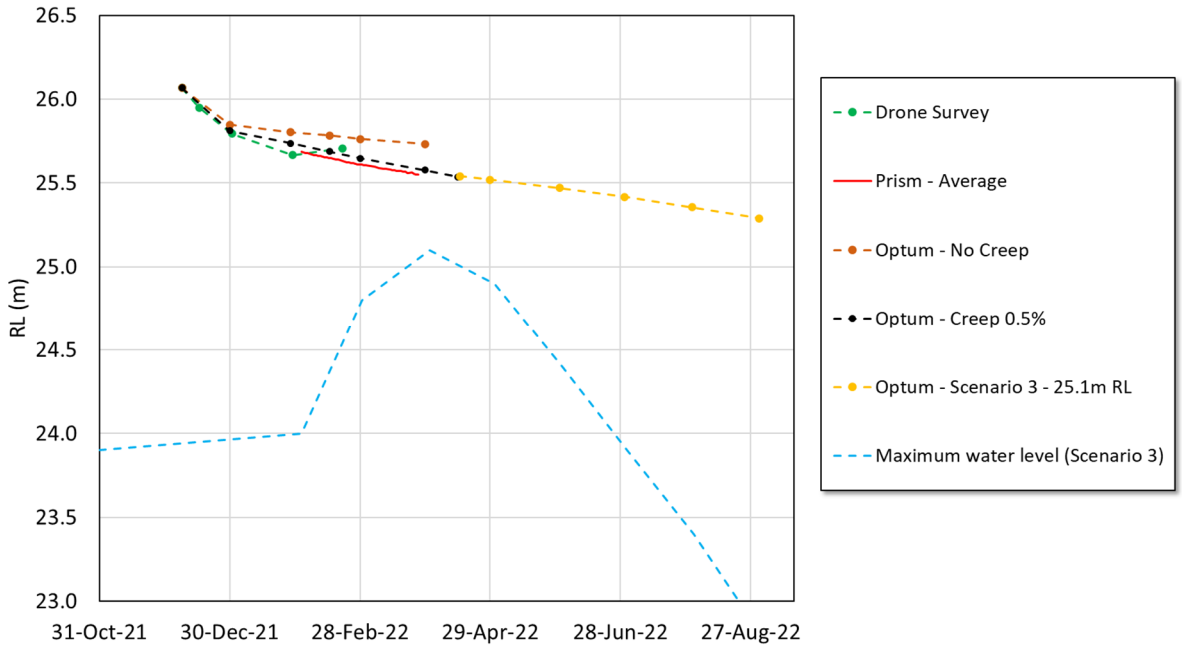

Figure 16 Settlement results compared to monitored settlement and predicted maximum decant water level

However, due to the presence of creep, it can be expected that the internal bund will continue to settle at a constant rate and that this settlement will be ongoing. Results indicate that the settlement rate will decrease slightly depending on operational factors (i.e. the operational level at the decant pond) but that the trend

remains constant. This negligible difference is attributed to the fact that the changes of vertical effective stress in the order of magnitude induced by the increase in pond levels are not of a material difference to the ongoing settlement. The numerical results coincide with the field-monitoring records, in which vertical deformation settlement governs the movement mechanism seen in the internal bund. Horizontal deformations are negligible and are attributed to the natural asymmetric conditions of field conditions.

4 Conclusion

Poorly managed and closed TSFs have wrought havoc in communities with devastating social, environmental and economic consequences. The industry is considered to be in crisis with the need to reduce TSF failures dramatically. Given the increasing demand placed on TSFs, with increasing volume and production directly leading to increasing pressures, properly managed closure of TSFs will play a critical role within the industry. Increasing confidence in the potential behaviour is essential to ensuring the integrity of closure designs, thus eliminating harm arising from TSF failure.

Deformation modelling has been used within this case study to highlight the potential role it may play in informing stakeholders of the potential behaviour of a TSF to allow for more informed decision-making. This deformation modelling has identified the core mechanism, informed by seepage modelling and onsite data collected from survey prisms. Creep was identified as a leading mechanism (assessed as being approximately 0.5% creep), resulting in ongoing vertical settlement.

The deformation modelling predictions matched with the results obtained from the survey prisms exceedingly well. Extending the model over the period of interest determined that a total displacement of approximately 1 m can be expected for the internal bund from the 3rd November 2021 until the 31st August 2022. A lower maximum decant pond level would result in a marginally lower settlement, but the order of magnitude is anticipated to be consistent with the prediction presented herein.

Assuming the maximum decant pond level were to be realised on the 15th April 2022, this corresponds to a further 0.25 m settlement leading out to the 31st August 2022. Based on these results, there would be a freeboard of approximately 500 mm when the decant pond is at its maximum elevation.

References

Australian National Committee on Large Dams 2019, *Guidelines on Tailings Dams: Planning, Design, Construction, Operation and Closure*, revision 1, Hobart.

Bowker, LN & Chambers, DM 2015, 'The risk, public liability, & economics of tailings storage facility failures', *Earthwork Act*, vol. 24, pp. 1–56.

Bruschi, GJ, Fante, F, Araújo, MTD, Macedo, GD & Ruver, CA 2021, 'Analysis of different failure criteria to evaluate bauxite tailings mechanical behavior through numerical modelling', *Soils and Rocks,* vol. 44.

Espinoza, RD & Morris, JW 2017, 'Towards sustainable mining (part II): accounting for mine reclamation and post reclamation care liabilities', *Resources Policy*, vol. 52, pp.29–38.

Hu, W, Xin, CL, Li, Y, Zheng, YS, van Asch, TWJ & McSaveney, M 2021, 'Instrumented flume tests on the failure and fluidization of tailings dams induced by rainfall infiltration', *Engineering Geology*, vol. 294, p. 106401.

International Commission on Large Dams 2017, 'Tailings dam design: technology update (ICOLD Bulletin)', *Proceedings of the 85th Annual Meeting of International Commission on Large* Dams, Czech National Committee on Large Dams.

Mánica, MA, Marcos A, Antonio G & Lluis M 2022, 'Application of a critical state model to the Merriespruit tailings dam failure', *Proceedings of the Institution of Civil Engineers-Geotechnical Engineering*, vol. 175, no. 2, pp. 151–165.

Mesri, G & Castro, A 1987, 'C α/C c concept and K 0 during secondary compression', *Journal of Geotechnical Engineering*, vol. 113, no. 3, pp. 230–247.

Mining Association of Canada 2017, 'A guide to the management of tailings facilities', 3rd edn, Ottawa.

Rico, M, Benito, G & Diez-Herrero, A 2008, 'Floods from tailings dam failures', *Journal of Hazardous Materials*, vol. 154, no. 1–3, pp. 79–87.

Roscoe, K & Burland, JB 1968, 'On the generalized generalised stress-strain behaviour of wet clay', in J Heyman & F Leckie (eds), *Engineering Plasticity*, Cambridge University Press, Cambridge, pp. 535–609.

Utomo, P, Syakur, P & Nikraz, HR 2009, 'A review on the performance of modified cam clay model in predicting the mechanical behaviour of heavily overconsolidated clay', *Media Teknik Sipil*, vol. 7, no. 1, p. 31.

Williams, DJ 2021, 'Lessons from tailings dam failures—where to go from here?', *Minerals*, vol. 11, no. 8, p. 853.